duced by changes in core temperature and hydrogen density would require a sizeable control system, and the rapid rate of change would require both a sensitive and a fast-acting control system. These stipulations may be difficult to fulfill.

There are ways to reduce the reactivity variation during start-up. An obvious method is to place a nuclear poison in the core to harden the thermal spectrum, which in turn reduces the change in nuclear properties induced by temperature variations. However, this procedure has the adverse side effect of reducing the external control rod worth by reducing the neutron leakage.

References

[1] Johnson, P. G., "Nuclear rocket applications," *Astronautics* **7**, no. 12, 22–27 (1962).

[2] Bogart, D. and Lantz, E., "Nuclear physics of solid-core gas-cooled rocket propulsion reactors," *Proceedings of the NASA-University Conference on the Science and Technology of Space Exploration*, Vol. 2, pp. 77–85, NASA SP-11 (November 1–3, 1962).

[3] Mohler, R. R. and Perry, J. E., Jr., "Nuclear rocket engine control," *Nucleonics* **19**, no. 4, 80–84 (1961).

[4] Plebuch, R. K., "Reactor physics of nuclear rocket reactors," Sc.D. Thesis, Dept. of Nuclear Engineering, Massachusetts Institute of Technology (1963).

[5] Meghreblian, R. V. and Holmes, D. K., *Reactor Analysis* (McGraw-Hill Book Co., Inc., New York, 1960), pp. 750–752.

[6] Joanou, G. D. and Dudek, J. S., "GAM-I: Calculation of fast group neutron spectra," General Atomics, San Diego, Calif., Rept. GA-1850 (June 1961).

[7] Cohen, E. R., "Neutron velocity spectrum in a heavy moderator," *Nucl. Sci. Eng.* **2**, 227–245 (1957).

[8] Ellerbrock, H. H., Liningood, J. N. B., and Straight, D. M., "Fluid flow and heat transfer problems in nuclear rockets," *Proceedings of the NASA-University Conference on the Science and Technology of Space Exploration*, Vol. 2, pp. 87–116, NASA SP-11 (November 1–3, 1962).

Rocket Motor with Electric Acceleration in the Throat

JAN ROSCISZEWSKI*
General Dynamics/Astronautics, San Diego, Calif.

PRESENT rocket motors seem to be inadequate for long space missions because of poor mass utilization due to limited exhaust velocity (low specific impulse $I_{sp} < 500$ sec). One can obtain much better mass utilization by using the concept of electric propulsion (I_{sp} of the order of 10,000). However, for intermediate specific impulses around 1000 to 2000, the combination of both seems to be adequate. The chemical process in the combustion chamber will provide high enough electric conductivity by adding seeding substance (1% potassium or cesium). The gas is accelerated to the sonic speed in the convergent nozzle (Fig. 1), then, in the straight channel with segmented electrodes and the normal magnetic and applied electric fields, it is accelerated to supersonic speed with relatively small pressure drop. Final expansion occurs in the divergent nozzle. The location of the electric accelerator in the throat offers the following advantages: 1) high enough temperature and therefore sufficient electric conductivity, and 2) minimum spacing between magnetic field coils. The present scheme requires a separate energy source that must be a nuclear power generator.
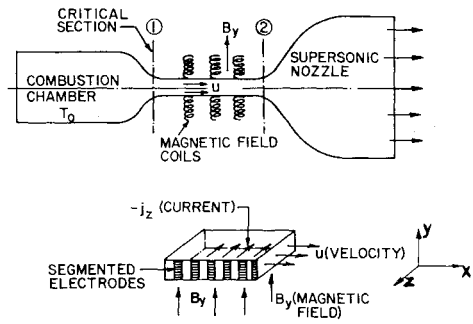
Fig. 1   Rocket motor with electric acceleration in the throat.

Fundamental Equations

Assuming one-dimensional flow at low magnetic Reynolds number one obtains

Conservation of Mass

$$\rho u = \rho_1 u_1 = \text{const} \tag{1}$$

where u denotes velocity, ρ is density, and subscript 1 denotes reference parameters.

Conservation of Momentum

$$\rho u (du/dx) + (dp/dx) = -j_z B_y \tag{2}$$

where the right-hand side represents Lorentz force.

Conservation of Energy

$$\rho T \frac{DS}{Dt} = \frac{pu}{\gamma - 1}\left(\frac{1}{p}\frac{dp}{dx} - \frac{\gamma}{\rho}\frac{d\rho}{dx}\right) = \frac{j_z^2}{\sigma} \tag{3}$$

or

$$\gamma p \frac{du}{dx} + u \frac{dp}{dx} = (\gamma - 1)\frac{j_z^2}{\sigma} \tag{3'}$$

The terms j_z^2/σ represent joule heating (i_z is current density, and σ is electric conductivity).

Ohm's Law

$$j_z = -\sigma(E - uB_y) \tag{4}$$

where E_z is an applied electric field, and B_y is the magnetic field.

The following dimensionless variables are introduced:

$$M_1 = \frac{u_1}{a_1} \qquad \bar{u} = \frac{u - u_1}{a_1} \qquad \bar{p} = \frac{p}{p_1} \qquad \bar{a} = \frac{a}{a_1}$$

(velocity of sound ratio)

$$\bar{j} = \frac{j_z}{\sigma B_y a_1} \qquad \Lambda = \frac{E_z}{B_y a_1} \qquad \xi = \frac{a_1 B_y^2 \int \sigma dx}{p_1}$$

The introduction of ξ makes the foregoing equations independent of the conductivity σ and its variation with temperature. However, the effective physical distance depends on σ.

Equations (2–4) can be written in the forms

$$\gamma M_1 (d\bar{u}/d\xi) + (d\bar{p}/d\xi) = -\bar{j} \tag{5}$$

$$\gamma \bar{p} \frac{d\bar{u}}{d\xi} + (M_1 + \bar{u})\frac{d\bar{p}}{d\xi} = (\gamma - 1)\bar{j}^2 \tag{6}$$

$$\bar{j} = M_1 + \bar{u} - \Lambda \tag{7}$$

From Eq. (1) the velocity of sound is

$$a = \{\bar{p}[1 + (u/M_1)]\}^{1/2} \tag{8}$$

From Eqs. (5) and (6) one gets

$$\frac{d\bar{u}}{d\xi} = \frac{-(M_1 + \bar{u})\bar{j} + (\gamma - 1)\bar{j}^2}{\gamma M_1(M_1 + \bar{u}) - \gamma \bar{p}} \tag{9}$$
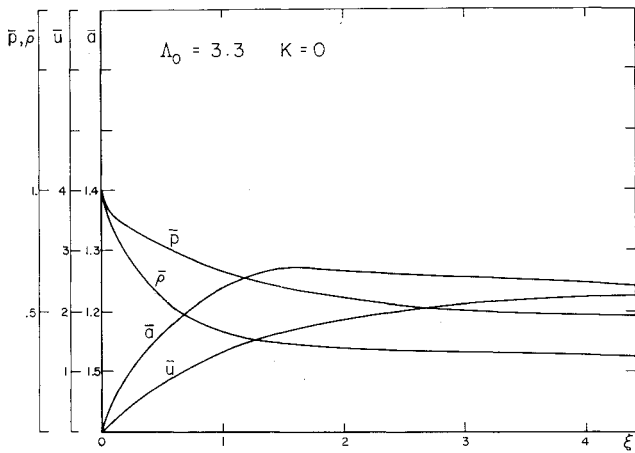
Fig. 2   Flow characteristics along the $j \times B$ accelerator $\Lambda_0 = E_{z0}/B_y a_1 = 3.3$, $K = 0$.
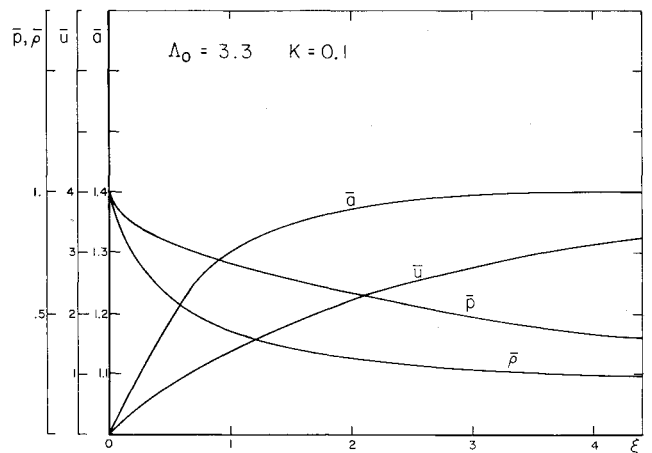

Fig. 3   Flow characteristics along the $j \times B$ accelerator $\Lambda_0 = 3.3$, $K = 0.1$.

or, using (7),

$$\frac{d\bar{u}}{d\xi} = \frac{\Lambda - M_1 - \bar{u}}{\gamma} \frac{(\gamma - 1)\Lambda - \gamma(M_1 + \bar{u})}{\bar{p} - M_1(M_1 + \bar{u})} \quad (10)$$

Similarly,

$$\frac{d\bar{p}}{d\xi} = (\Lambda - M_1 - u) \frac{\bar{p} - (\gamma - 1)(\Lambda - M_1 - \bar{u})M_1}{\bar{p} - M_1(M_1 + \bar{u})} \quad (11)$$

From Eqs. (10) and (11),

$$\frac{d\bar{p}}{d\bar{u}} = \gamma \frac{\bar{p} - (\gamma - 1)(\Lambda - M_1 - \bar{u})M_1}{\gamma(\Lambda - M_1 - \bar{u}) - \Lambda} \quad (12)$$

At the critical section $M_1 = 1$, $\bar{p} = 1$, $\bar{u} = 0$, $du/d\xi = \infty$, and $dp/d\xi = \infty$; however, dp/du and $du^2/d\xi$ are finite. Multiplying Eq. (10) by $\bar{u}$, one gets for $\bar{u} = 0$ (applying the l'Hospital rule)

$$\frac{d\bar{u}^2}{d\xi}\bigg|_{\xi=0} = 2 \frac{\Lambda - 1}{\gamma} \frac{(\gamma - 1)\Lambda - \gamma}{(dp/du)|_{\xi=0} - 1}$$

or, using Eq. (12),

$$\frac{d\bar{u}^2}{d\xi}\bigg|_{\xi=0} = 2 \frac{\Lambda - 1}{\gamma} \times$$
$$\frac{(\gamma - 1)\Lambda - \gamma}{\gamma\{1 - (\gamma - 1)(\Lambda - 1)/[\gamma(\Lambda - 1) - \Lambda]\} - 1} =$$
$$2 \frac{-(\Lambda - 1)[(\gamma - 1)\Lambda - \gamma]}{\gamma(\gamma + 1)} \quad (13)$$

To obtain accelerated flow

$$(d\bar{u}^2/d\xi|_{\xi=0} > 0) \qquad 1 < \Lambda < \gamma/(\gamma - 1)$$

In other words, the electric field at the critical section can not be too large. The explanation of this fact is that there are two opposing effects: gas acceleration due to Lorentz force (proportional to $\bar{j}$) and heat generation due to joule heating (proportional to $\bar{j}^2$).

It is well known that, to accelerate the gas in a straight tube in subsonic flow, heat should be put in, but in supersonic flow heat should be extracted. Joule heating will therefore oppose the acceleration due to Lorentz force, and for high enough current level there will be no acceleration, $du^2/d\xi = 0$. From Eq. (13),

$$u^2|_{\xi=\Delta\xi} = -2 \frac{\Lambda - 1}{\gamma} \frac{[(\gamma - 1)\Lambda - \gamma]}{\gamma(\gamma + 1)} \Delta\xi \quad (14)$$

and Eqs. (10) and (12) give velocity and pressure as a function of the distance.

Equation (8) gives velocity of sound, and Eq. (1) gives the density ratio

$$\rho/\rho_1 = M_1/(\bar{u} + 1) \quad (15)$$

and temperature ratio (R = const)

$$\bar{T} = T/T_1 = \bar{p}\rho_1/\rho = (\bar{p}/M_1)(\bar{u} + 1) \quad (16)$$

For Λ = const, the limiting velocity is ($du/d\xi = 0$)

$$u = (\Lambda - 1) \quad \text{for} \quad \Lambda = 3.3 \qquad u_{\lim} = 2.3$$

Further increase of velocity will take place in the divergent nozzle. To obtain higher velocity, variable Λ and segmented electrodes both could be applied. However, to have small axial current, the electric field variation can not be large.

Equations (10) and (11), with the initial step using Eqs. (14) and (12), have been solved on an IBM 7090 computer. The results are presented in Figs. 2–4 as a function of dimensionless variable ξ. The results are presented for Λ being the linear function of the dimensionless variable ξ:

$$\Lambda = \Lambda_0(1 + K\xi) = 3.2(1 + K\xi)$$

Using the isentropic flow relations one can calculate the maximum velocity (flow into vacuum)

$$u_{\max} = [u_2^2 + 2a_2^2/(\gamma - 1)]^{1/2}$$

where u_2, a_2 are velocity and speed of sound at the end of the accelerator. The results are plotted in Figs. 2–4 for $K = 0.1$ and 0.5, respectively. For $K = 0$ and $\gamma = 1.4$, we find $u_2 = 2.25$ and $a = 1.25$. The maximum velocity is $\bar{u}_{\max} = 3.6$, or
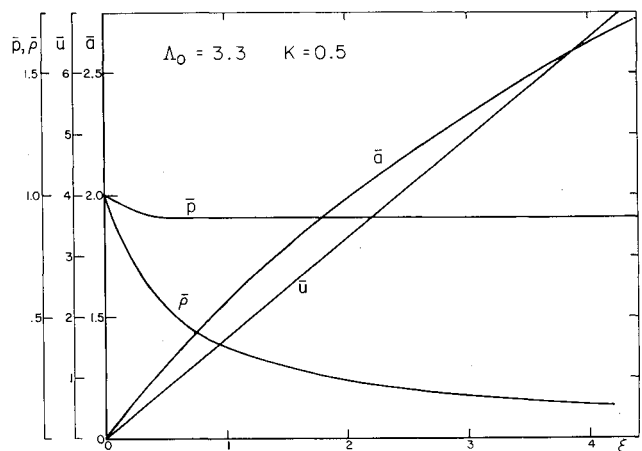

Fig. 4   Flow characteristics along the $j \times B$ accelerator $\Lambda_0 = 3.3$, $K = 0.5$.

about 50% larger than the maximum velocity without electric acceleration, $\bar{u}_{max} = [(\gamma + 1)/(\gamma - 1)]^{1/2} = 2.45$.

Dimensionless distance $\xi = 4.53$ or for $\sigma = 200$ mho/m $=$ const and $B_y = 10,000$ gauss, $a_1 = 1200$ m/sec, $p_1 = 10$ atm, and $x = 1.87$ m; at $B_y = 20,000$ gauss, $x = 0.47$ m. At $K = 0.1$ and $\xi = 4.2$, $\bar{u}_2 = 3.2$, $a_2 = 1.4$, and $u_{max} = 4.47$. At $K = 0.5$ and $\xi = 3.95$: $\bar{u}_2 = 6.5$, $a_2 = 2.6$, and $u_{max} = 8.7$.

Automatic Control Systems for Ion Engines

R. M. Worlock,[*] A. T. Forrester,[†]
G. W. Purmal,[‡] A. M. Schneider,[§] and G. Sohl[¶]
Electro-Optical Systems, Inc., Pasadena, Calif.

Contact Engine System

THE contact engine control system performs the following tasks: 1) upon command, starts up the engine and brings it to a predetermined level of operation, 2) maintains thrust at a predetermined level and controls ionizer temperature according to a criterion to be described, and 3) upon command shuts down the engine.

The start-up sequence is very simple; at $t = 0$, power is applied to feed system heaters and to the ionizer heater. When feed system and ionizer reach operating temperature, engine operation is begun by applying high voltage to the engine and closing the thrust stabilization feed-back loop. Since the engine operates at a fixed positive accelerating potential, the thrust produced is determined by the value of ion beam current. The thrust control loop operates by measuring the beam current, which is taken to be the algebraic sum of the currents from the positive and negative high-voltage power supplies, comparing this measurement with a reference signal, amplifying the difference, and applying it to the controlling element of the cesium vapor feed system.

To protect the engine against damage from excessive accelerator electrode drain currents, the constraint that accelerator current not exceed some reference value has been incorporated into the beam-current control loop. If the accelerator current exceeds the reference value, a signal proportional to the difference is introduced into the loop. This decreases the beam current, which in turn decreases the accelerator drain current. The result is a control loop that stabilizes beam current at a reference value or at a value that results in a predetermined value of accelerator drain current, whichever is smaller.

Mild sparking in the engine can be tolerated by the power supplies and does not appear to be damaging to the engine. Larger discharges activate the power supply overload detectors, which turn off both supplies for a few tenths of a second and then turn them both back on again. If repetitive over-

loading occurs, the supplies and the vapor feed are turned off for about a minute and then turned back on.

Optimum control of the ionizer temperature involves a compromise between competing factors. If the ionizer temperature is too high, radiated power losses are excessive. If the ionizer temperature is too low, other power losses begin to be important, and long-term stable operation is jeopardized. Thus it is important to maintain ionizer temperature at an "optimum" value derived according to some predetermined criterion.

Such a criterion can be based on the relation between ionizer temperature and the neutral efflux, i.e., that portion of the cesium fed into the ionizer which escapes without having been ionized. The neutral efflux-ionizer temperature relation is characterized by a very steeply rising part, a "knee," and a relatively flat part. Optimum operation occurs in the vicinity of the knee; on the low-temperature side, the neutral efflux is excessive, and on the other, excessive heater power is required to produce a slight additional decrease in neutral efflux. The function of the control system is to keep the engine operating at the knee of the curve. In the system that has been built and tested, the operating point is defined by a value of the derivative of neutral efflux with respect to temperature.

The derivative is determined by square wave modulating the ionizer heater power and making measurements on the resulting varying neutral efflux signal. Because of the fluctuations such as engine sparking, this signal is relatively noisy, making it necessary to take care in making measurements of signal amplitude. The system developed makes use of synchronous detection; a block diagram of the control loop is shown in Fig. 1 and typical waveforms are shown in Fig. 2. The neutral detector output (waveform 1 of Fig. 2) consists of a background level upon which is superimposed the variation due to ionizer temperature modulation. The modulation period is 80 sec and the thermal time constant of the ionizer, the dominant time constant in the system, is about 300 sec. The inverter produces the waveform 2 by inverting half of each cycle. At $t = 0$ (shown in waveform 7) the integrator is reset to zero and starts integrating to produce waveform 3. By integrating over the period indicated, the integrator output at $t = t_2$ is the integral of the absolute value of the alternating component of the neutral detector signal, less a fixed amount, which is the integral of the reference signal. Any noise appearing in the neutral detector signal is now integrated and produces much smaller output fluctuations. Furthermore, pairs of noise pulses occurring during the two halves of the integration cycle tend to cancel. At $t = t_2$, the sampler transmits the integrator output (waveform 3) and the compensator output (waveform 6) to the hold circuit (waveform 4), which produces output (waveform 5). The compensator output adjusts to equal the new level of the hold-circuit output during the next cycle, thus acting as a storage unit, enabling the control loop to regulate with zero steady-
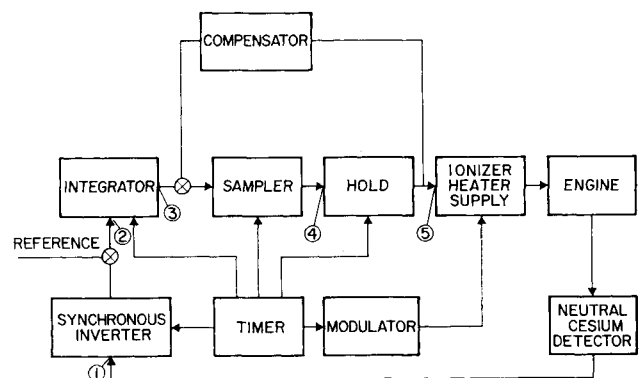

Fig. 1 Ionizer temperature control loop.